

# A guided network propagation approach to identify disease genes that combines prior and new information

Borislav H. Hristov, Bernard Chazelle and Mona Singh<sup>\*†</sup>

## Abstract

A major challenge in biomedical data science is to identify the causal genes underlying complex genetic diseases. Despite the massive influx of genome sequencing data, identifying disease-relevant genes remains difficult as individuals with the same disease may share very few, if any, genetic variants. Protein-protein interaction networks provide a means to tackle this heterogeneity, as genes causing the same disease tend to be proximal within networks. Previously, network propagation approaches have spread “signal” across the network from either known disease genes *or* genes that are newly putatively implicated in the disease (e.g., found to be mutated in exome studies or linked via genome-wide association studies). Here we introduce a general framework that considers both sources of data within a network context. Specifically, we use prior knowledge of disease-associated genes to guide random walks initiated from genes that are newly identified as perhaps disease-relevant. In large-scale testing across 24 cancer types, we demonstrate that our approach for integrating both prior and new information not only better identifies cancer driver genes than using either source of information alone but also readily outperforms other state-of-the-art network-based approaches. To demonstrate the versatility of our approach, we also apply it to genome-wide association data to identify genes functionally relevant for several complex diseases. Overall, our work suggests that guided network propagation approaches that utilize both prior and new data are a powerful means to identify disease genes.

---

<sup>\*</sup>Department of Computer Science and Lewis-Sigler Institute for Integrative Genomics, Princeton University

<sup>†</sup>Email mona@cs.princeton.edu

## Introduction

Large-scale efforts such as the 1000 Genomes Project [1], The Cancer Genome Atlas (TCGA) [2], and the Genome Aggregation Database [3], among others, have catalogued millions of variants occurring in tens of thousands of healthy and disease genomes. Despite this abundance of genomic data, however, understanding the genetic basis underlying complex human diseases remains challenging [4]. In contrast to simple Mendelian diseases, for which a small set of commonly shared genetic variants are responsible for disease phenotypes, complex heterogeneous diseases are driven by a myriad of combinations of different alterations. Individuals exhibiting the same phenotypic outcome—a particular disease—may share very few, if any, genetic variants, thereby making it difficult to discover which of numerous variants are associated with heterogeneous diseases, even when focusing just on changes that occur within genes.

Biological networks provide a powerful, unifying framework for identifying disease genes [5–8]. Genes relevant for a given disease typically target a relatively small number of biological pathways, and since genes that take part in the same pathway or process tend to be close to each other in networks [9, 10], disease genes cluster within networks [11, 12]. Consequently, if genes known to be causal for a particular disease are mapped onto a network, other disease-relevant genes are likely to be found in their vicinity [13]. Thus, the signal from known disease genes can be “propagated” across a network to prioritize either all genes within the network or just candidate genes within a genomic locus where single nucleotide polymorphisms have been correlated with an increased susceptibility to disease [14–19].

While initial network approaches to identify disease genes focused on propagating knowledge from a set of known “gold standard” disease genes, with the widespread availability of cancer sequencing data and genome-wide association studies (GWAS), the source of where information is propagated from has shifted to genes that are newly identified as perhaps playing a role in disease [20–26]. For example, in the cancer context, diffusing a signal from genes that are somatically mutated across tumors is highly effective for identifying cancer-relevant genes and pathways [21, 25]; notably, while frequency-based approaches identify genes that “drive” cancer by searching for those that are recurrently mutated across tumor samples beyond some background rate [27], such a network propagation approach can even pinpoint rarely mutated driver genes if they are within subnetworks whose component genes, when considered together, are frequently mutated.

Thus there are two dominant network propagation paradigms for uncovering disease genes: spreading signal either from well-established, annotated disease genes or from genes that have some new evidence of being disease-relevant. While both have been successful independently, we argue that both sources of information should be utilized together, and that existing knowledge of disease genes should inform the way new data is examined within networks. That is, while our prior knowledge of causal genes for a given disease may be incomplete, it nevertheless is a valuable source of information about the biological processes underlying the disease; furthermore, in many cases, there is substantial prior knowledge and there is no reason disease gene discovery should proceed *de novo* from newly observed alterations.

In this paper, we introduce a guided network propagation framework to uncover disease genes, where signal is propagated from new data so as to tend to move towards genes that are closer to known disease genes. Our core method of propagating information within a network is via either diffusion [28] or random walks with restarts (RWRs) [14], as these are mathematically sound, well-established approaches, where numerical solutions are easily obtained. In particular, our approach first diffuses a signal from known disease genes, and then performs either guided random walks or guided diffusion from the new data so as to preferentially move towards genes that have received higher amounts of signal from the initial set of known disease genes. In contrast, previous network propagation methods for disease gene discovery have performed diffusion or random walks uniformly from each node (i.e., in an “unguided” manner, as in e.g., [21, 24]), or where the diffusion is scaled by weights on network edges that reflect their estimated reliabilities (e.g., [23]). Alternatively, several approaches have attempted to uncover disease genes by explicitly connecting in the

network genes that have genetic alterations with genes that have expression changes [29–34]; while well-suited for finding genes causal for observed expression changes, such approaches are less appropriate as a means to link prior and new information, and our approach instead uses prior knowledge to simply influence information propagation within the network.

We demonstrate the efficacy of our method **uKIN**—**using Knowledge In Networks**—by first applying it to discover genes causal for cancer. Here, new information consists of genes that are found to be somatically mutated in tumors—only a small number of which are thought to play a functional role in cancer—and prior information is comprised of subsets of “driver” genes known to be cancer-relevant [35]. In rigorous large-scale, cross-validation style testing across 24 cancer types, we demonstrate that propagating signal by integrating both these sources of information performs substantially better in uncovering known cancer genes than propagating signal from either source alone. Notably, even using just a small number of known cancer genes (5–20) to guide the network propagation from the set of mutated genes results in substantial improvements over the unguided approach. Next, we compare **uKIN** to four state-of-the-art network-based methods that use somatic mutation data for cancer gene discovery and find that **uKIN** readily outperforms them, thereby demonstrating the advantage of additionally incorporating prior knowledge. We also show that by using cancer-type specific prior knowledge, **uKIN** can better uncover causal genes for specific cancer types. Finally, to showcase **uKIN**’s versatility, we show its effectiveness in identifying causal genes for three other complex diseases, where the genes known to be associated with the disease come from the Online Mendelian Inheritance in Man (OMIM) [36] and genes comprising the new information arise from genome-wide association studies (GWAS).

## Methods

**Overview.** At a high level, our approach **uKIN** propagates new information across a network, while using prior information to guide this propagation (Figure 1). While our approach is generally applicable, here we focus on the case of propagating information across biological networks in order to find disease genes. We assume that prior knowledge about a disease consists of a set of genes already implicated as causal for that disease, and new information consists of genes that are potentially disease-relevant. In the scenario of uncovering cancer genes, prior information comes from the set of known cancer genes, and new information corresponds to those genes that are found to be somatically mutated across patient tumors. For other complex diseases, new information may arise from (say) genes weakly associated with a disease via GWAS studies or found to have *de novo* or rare mutations in a patient population of interest.

The first step of our approach is to compute for each gene a measure that captures how close it is in the network to the prior knowledge set of genes  $\mathcal{K}$  (Figure 1a). To accomplish this, we spread the signal from the genes in  $\mathcal{K}$  using a diffusion kernel [28]. Next, we consider new information consisting of genes  $\mathcal{M}$  that have been identified as potentially being associated with the disease. As we expect those that are actually disease-relevant to be proximal to each other and to the previously known set of disease genes, we spread the signal from these newly implicated genes  $\mathcal{M}$ , biasing the signal to move towards genes that are closer to the known disease genes  $\mathcal{K}$  (Figure 1b). We accomplish this by performing RWRs, where with probability  $\alpha$ , the walk jumps back to one of the genes in  $\mathcal{M}$ . That is,  $\alpha$  controls the extent to which we use new versus prior information, where higher values of  $\alpha$  weigh the new information more heavily. With probability  $1 - \alpha$ , the walk moves to a neighboring node, but instead of moving from one gene to one of its neighbors uniformly at random as is typically done, the probability instead is higher for neighbors that are closer to the prior knowledge set of genes  $\mathcal{K}$ . Genes that are visited more frequently in these random walks are more likely to be relevant for the disease because they are more likely to be part of important pathways around  $\mathcal{K}$  that are also close to  $\mathcal{M}$ . We thus numerically compute the probability with which each gene is visited in these random walks, and then use these probabilities to rank the genes. As an alternative to a

RWR, we also experiment with implementing the guided propagation via a diffusion kernel [28]. Each step of our procedure is described in more detail below.

**Notation.** The biological network is modeled as an undirected graph  $G = (V, E)$  where each vertex represents a gene, and there is an edge between two vertices if an interaction has been found between the corresponding protein products. We require  $G$  to be connected, restricting ourselves to the largest connected component if necessary. We explain our formulation with respect to cancer, but note that it is applicable in other settings (both disease and otherwise). The set of genes already known to be cancer associated is denoted by  $\mathcal{K} = \{k_1, k_2, \dots, k_l\}$ . The set of genes that have been found to be somatically mutated in a cohort of individuals with cancer is denoted by  $\mathcal{M} = \{m_1, m_2, \dots, m_p\}$ , with  $\mathcal{F} = \{f_{m_1}, f_{m_2}, \dots, f_{m_p}\}$  corresponding to the rate with which each of these genes is mutated. We refer to  $\mathcal{K}$  as the prior knowledge and  $\mathcal{M}$  as the new information. We assume that  $\mathcal{K} \subset V$  and  $\mathcal{M} \subset V$ ; in practice, we remove genes not present in the network. The genes within  $\mathcal{K}$  and  $\mathcal{M}$  may overlap (i.e., it is not required that  $\mathcal{K} \cap \mathcal{M} = \emptyset$ ).

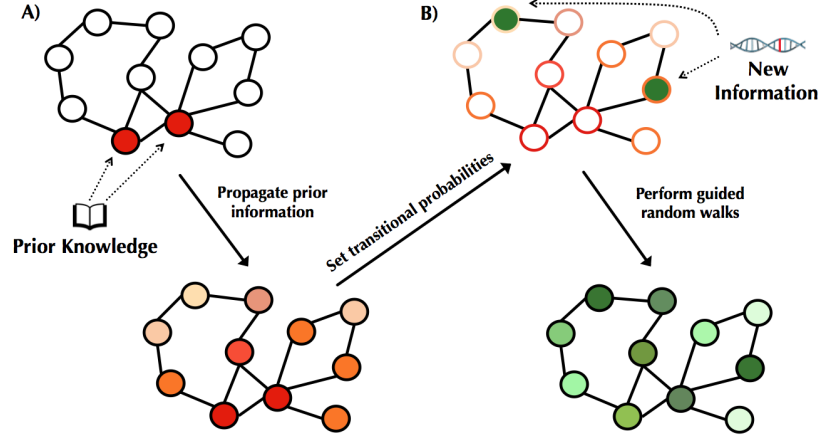


**Figure 1: Overview.** (a) Known disease-relevant genes (prior knowledge) are mapped onto an interaction network (shown in red, top). Signal from this prior knowledge is propagated through the network via a diffusion approach [28], resulting in each gene in the network being associated with a score such that higher scores (visualized in darker shades of red, bottom) correspond to genes closer to the set of known disease genes. These scores are used to set transition probabilities between genes such that a neighboring gene that is closer to the set of prior knowledge genes is more likely to be chosen. (b) Genes putatively associated with the disease—corresponding to the new information—are mapped onto the network (shown in green, top). To integrate both sources of information, RWRs are initiated from the set of putatively associated genes, and at each step, the walk either restarts or moves to a neighboring gene according to the transition probabilities (i.e., walks tend to move towards genes outlined in darker shades of red). These prior-knowledge “guided” RWRs have a stationary distribution corresponding to how frequently each gene is visited, and this distribution is used to order the genes. Higher scores correspond to more frequently visited genes (depicted in darker greens, bottom).

**Guided RWR Algorithm.** For each gene  $i \in V$ , assume that we have a measure  $q_i$  that represents how close  $i$  is to the set of genes  $\mathcal{K}$ . We will use the nonnegative vector  $q$ , which we describe in the next section, to guide a random walk starting at the nodes in  $\mathcal{M}$  and walking towards the nodes in  $\mathcal{K}$ . Each walk starts from a gene  $i$  in  $\mathcal{M}$ , chosen with probability proportional to its mutational rate  $f_i$ . At each step, with probability  $\alpha$  the walk can restart from a gene in  $\mathcal{M}$ , and with probability  $1 - \alpha$  the walk moves to a neighboring gene picked probabilistically based upon  $q$ . Specifically, if  $\mathcal{N}(i)$  are the neighbors of node  $i$ , the walk goes from node  $i$  to node  $j \in \mathcal{N}(i)$  with probability proportional to  $q_j / \sum_{k \in \mathcal{N}(i)} q_k$ . That is, if at time  $t$  the walk is at node  $i$ , the probability that it transitions to node  $j$  at time  $t + 1$  is

$$p_{ij} = (1 - \alpha)\delta_{ij} \cdot \frac{q_j}{\sum_{k \in \mathcal{N}(i)} q_k} + \alpha \cdot \frac{f_j}{\sum_{k \in \mathcal{M}} f_k}$$

where  $\delta_{ij} = 1$  if  $j \in \mathcal{N}(i)$  and 0 otherwise. Hence, the guided random walk is fully described by a

stochastic transition matrix  $P$  with entries  $p_{ij}$ . By the Perron-Frobenius theorem, the corresponding random walk has a stationary distribution  $\pi$  (a left eigenvector of  $P$  associated with the eigenvalue 1). If the graph  $G$  is connected, then the back edges to  $\mathcal{M}$  easily ensure that  $\pi$  is unique and can be approximated by a long enough random walk. For each gene  $i$ , its score is given by the  $i$ th element of  $\pi$ . The genes whose nodes have high scores are most frequently visited and, therefore, are more likely relevant to cancer as they are close to both the mutated starting nodes as well as to known cancer genes.

**Incorporating prior knowledge.** For each gene in the network, we wish to compute how close it is to the set of cancer-associated genes  $\mathcal{K}$ . While many approaches have been proposed to compute “distances” in networks, we use a network flow/diffusion technique where each node  $k \in \mathcal{K}$  introduces a continuous unitary flow which diffuses uniformly across the edges of the graph and is lost from each node  $v \in V$  in the graph at a constant first-order rate  $\lambda$  [28]. Briefly, let  $A = (a_{ij})$  denote the adjacency matrix of  $G$  (i.e.,  $a_{ij} = 1$  if  $(i, j) \in E$  and 0 otherwise) and let  $S$  be the diagonal matrix where  $s_{ii}$  is the degree of node  $i \in V$ . Then, the Laplacian of the graph  $G$  shifted by  $\lambda$  is defined as  $L = S + \lambda I - A$ . The equilibrium distribution of fluid density on the graph is computed as  $q = L^{-1}b$  [28], where  $b$  is the vector with 1 for the nodes introducing the flow and 0 for the rest (i.e.,  $b_i = 1$  if  $v_i \in \mathcal{K}$  and  $b_i = 0$  if  $v_i \notin \mathcal{K}$  for  $\forall v_i \in V$ ). Note that  $L$  is diagonally dominant, hence nonsingular, for any  $\lambda \geq 0$ . We set  $\lambda = 1$  in our applications. The vector  $q$  can be efficiently computed numerically. Thus, at equilibrium, each node  $i$  in the graph is associated with a score  $q_i$  which reflects how close it is to the nodes already marked as causal for cancer.

**Guided diffusion.** Instead of performing RWRs to propagate knowledge in a guided manner, it is also possible to adapt the diffusion approach just outlined by letting  $A = (a_{ij})$  be defined such that  $a_{ij} = q_j / \sum_{k \in \mathcal{N}(i)} q_k$ , and using  $A$  to compute  $L$  and the equilibrium density as above.

**Data sources and pre-processing.** We test uKIN on two protein-protein interaction networks: *HPRD* (Release 9.041310) [37] and *BioGrid* (Release 3.2.99, physical interactions only) [38]. We pre-process the networks as in [39]. Briefly, we remove all proteins with an unusually high number of interactions ( $> 900$  interactions,  $> 10$  standard deviations away from the mean number of interactions). Additionally, to remove spurious interactions, we remove those that have a  $Z$ -score normalized diffusion state distance  $> 0.3$  [40]. This leaves *HPRD* with 9,379 proteins and 36,638 interactions and *BioGrid* with 14,326 proteins and 102,552 interactions.

We use level 3 cancer somatic mutation data from TCGA [2] for 24 cancer types (Supplemental Table 1). For each cancer type, we process the data as previously described and exclude samples that are obvious outliers with respect to their total number of mutated genes [39]. Our set of prior knowledge is constructed from the 719 CGC genes that are labeled by COSMIC (version August 2018) as being causally implicated in cancer [35]. For each cancer type, our new information consists of genes that have somatic missense or nonsense mutations, and we compute the mutational frequency of a gene as the number of observed somatic missense and nonsense mutations across tumors, divided by the number of amino acids in the encoded protein.

We obtain 24, 28, and 63 genes associated with three complex diseases, *age-related macular degeneration (AMD)*, *Amyotrophic lateral sclerosis (ALS)* and *epilepsy*, respectively, from OMIM [36]. These genes are used to construct the set of prior knowledge. For each disease, we form the set  $\mathcal{M}$  by querying from the GWAS database [41] the genes implicated for the disease and using the corresponding  $p$ -values to compute the starting frequencies  $f$ . Specifically, for each disease, for each GWAS study  $i$ , if a gene  $j$ ’s  $p$ -value is  $p_{i,j}$ , we set its frequency to  $\log(p_{i,j}) / \sum_k \log(p_{i,k})$  and then for each gene average these frequencies over the studies.

**Performance evaluation.** To evaluate our method in the context of cancer, we subdivide the CGC genes that appear in our network into two subsets. We randomly draw from the CGCs 400 genes to form a set  $\mathcal{H}$  of positives that we aim to uncover. From the remaining 199 CGCs present in the network, we randomly draw a fixed number  $l$  to represent the prior knowledge  $\mathcal{K}$  and run our framework. As we consider an increasing

number of most highly ranked genes, we compute the fraction that are in the set  $\mathcal{H}$  of positives. All CGC genes not in  $\mathcal{H}$  are ignored in these calculations. Importantly, the genes in  $\mathcal{K}$  which are used to guide the network propagation are never used to evaluate the performance of  $\text{uKIN}$ . Note that this testing set up, which measures performance on  $\mathcal{H}$ , allows us to compare performance of  $\text{uKIN}$  when choosing prior knowledge sets of different size  $l$  from the CGC genes not in  $\mathcal{H}$ .

We also compute area under the precision-recall curves (AUPRCs). In this case, all CGC genes in  $\mathcal{H}$  are considered positives, all CGC genes not in  $\mathcal{H}$  are neutral (ignored), and all other genes are negatives. Though we expect that there are genes other than those already in the CGC that play a role in cancer, this is a standard approach to judge performance (e.g., see [24]) as cancer genes should be highly ranked. To focus on performance with respect to the top predictions, we compute AUPRCs using the top 100 predicted genes. To better estimate AUPRCs and account for the randomness in sampling, we repeatedly draw (10 times) the set  $\mathcal{H}$  and for each draw we sample the genes comprising the prior knowledge  $\mathcal{K}$  10 times. The final AUPRC results from averaging the AUPRCs across all 100 runs.

We compare  $\text{uKIN}$  on the cancer datasets to the frequency-based method *MutSigCV* 2.0 [42] and four network-based methods, *DriverNet* [30], *Muffinn* [43], *nCOP* [39] and *HotNet2* [25]. All methods are run on each of the 24 cancer types with their default parameters. *Muffinn*, *nCOP* and *HotNet2* are run on the same network as  $\text{uKIN}$ , whereas *MutSigCV* does not use a network and *DriverNet* instead uses an influence (i.e., functional interaction) graph and transcriptomic data (we use their default influence graph and provide as input TCGA normalized expression data). Since  $\text{uKIN}$  uses a subset of CGCs as prior knowledge, we ensure that all methods are evaluated with respect to the hidden sets  $\mathcal{H}$  (i.e., of CGCs not used by  $\text{uKIN}$ ). Though we could just consider performance with respect to one hidden set, considering multiple sets enables a better estimate of overall performance. For these comparisons,  $\text{uKIN}$  with  $\alpha = 0.5$  is run 100 times, as described above, with 20 randomly sampled genes comprising the prior knowledge, and evaluation is performed with respect to the genes in the hidden sets. All methods' AUPRCs are computed using the same randomly sampled test sets  $\mathcal{H}$  and averaged at the end. Since *HotNet2* outputs a set of predicted cancer-relevant genes and does not rank them, we cannot compute AUPRCs for it; instead we compute precision and recall for its output with respect to the test sets  $\mathcal{H}$  and compare to  $\text{uKIN}$ 's when considering the same number of top scoring genes.

To evaluate our method in the context of the three complex diseases, we subdivide evenly the set of OMIM genes associated with each disease into the prior knowledge set  $\mathcal{K}$  and the set of positives  $\mathcal{H}$ . As with the cancer data, we do this repeatedly (100 times) and average AUPRCs at the end.

## Results

We first apply our method  $\text{uKIN}$  to uncover cancer genes. Genes that have missense and nonsense somatic mutations comprise the new information, and random walks start from these genes with probability proportional to their mutation rates. We apply our approach to data from 24 cancer types, but showcase results for glioblastoma multiforme (GBM). All results in the main paper use the *HPRD* protein-protein interaction network [37], with results shown for *BioGrid* [38] in the Supplement.

**$\text{uKIN}$  successfully integrates prior knowledge and new information.** We compare  $\text{uKIN}$ 's performance when using both prior and new knowledge (RWRs with  $\alpha = 0.5$ ), to versions of  $\text{uKIN}$  using either only new information ( $\alpha = 1$ ) or only prior information ( $\alpha = 0$ ). Briefly, we use 20 randomly drawn CGCs to represent the prior knowledge  $\mathcal{K}$  and another 400 randomly drawn CGCs to be the hidden set  $\mathcal{H}$  of unknown cancer-relevant genes that we aim to uncover (see **Performance evaluation** for details). We repeat this process 100 times, each time spreading signal using the diffusion approach [28] before performing RWRs from the genes observed to be somatically mutated. For each run, we analyze the ranked list of genes output by  $\text{uKIN}$  as we consider an increasing number of output genes, and average across runs the fraction that are members of the hidden set  $\mathcal{H}$  consisting of cancer driver genes.

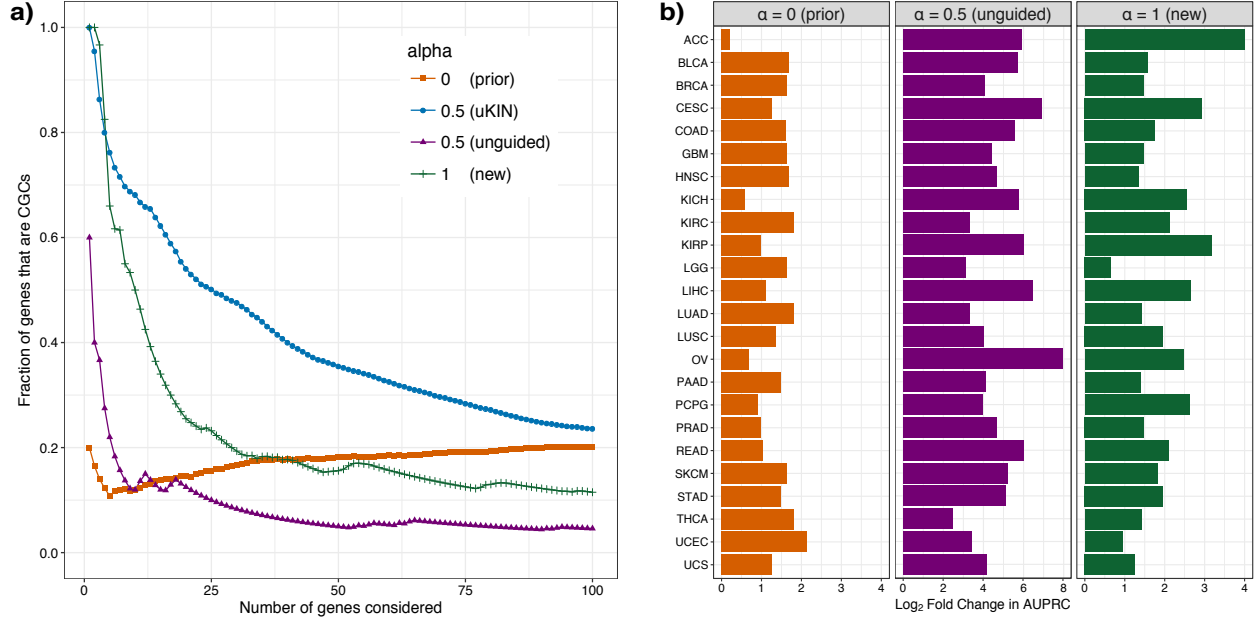


**Figure 2: uKIN successfully integrates new information and prior knowledge.** (a) We illustrate the effectiveness of our approach uKIN on the GBM data set and the HPRD protein-protein interaction network using 20 randomly drawn CGCs to represent the prior knowledge. We combine prior and new knowledge using a restart probability of  $\alpha = 0.5$  (blue line). As we consider an increasing number of high scoring genes, we plot the fraction of these that are part of the hidden set of CGCs. As baseline comparisons, we also consider versions of our approach where we use only the new information ( $\alpha = 1$ ) and order genes by their mutational frequency (green line); where we use new information to perform *unguided* random walks with  $\alpha = 0.5$  and order genes by their probabilities in the stationary distribution of the walk (which uses new information but not prior information, purple line); and where we use only prior information ( $\alpha = 0$ ) and order genes based on information propagated from the set of genes comprising our prior knowledge (orange line). Integrating both prior and new sources of information results in better performance. (b) The performance of uKIN when integrating information at  $\alpha = 0.5$  is compared to the three baseline cases where either only prior information is used ( $\alpha = 0$ , left) or when only new information is used ( $\alpha = 1$ , right and *unguided* RWRs with  $\alpha = 0.5$ , middle). In all three panels, for each cancer type, we plot the  $\log_2$  ratio of the AUPRC of uKIN with guided RWRs with  $\alpha = 0.5$  to the AUPRC of the other approach. Across all 24 cancer types, using both sources of information outperforms using just one source of information.

For  $\alpha = 0.5$ , we observe that a large fraction of the top predicted genes using the GBM dataset are part of the hidden set of known cancer genes (Figure 2a). At  $\alpha = 1$ , our method completely ignores both the network and the prior information  $\mathcal{K}$  and is equivalent to ordering the genes by their mutational frequencies. The very top of the list output by uKIN when  $\alpha = 1$  consists of the most frequently mutated genes (in the case of GBM, this includes *TP53* and *PTEN*). As we consider an increasing number of genes, ordering them by mutational frequency is clearly outperformed by uKIN with  $\alpha = 0.5$ . At the other extreme with  $\alpha = 0$ , the starting locations and their mutational frequencies are ignored as the random walk is memoryless and the stationary distribution depends only upon the propagated prior information  $q$ . As expected, performance is considerably worse than when running uKIN with  $\alpha = 0.5$ . Nevertheless, we observe that several CCGs are found for  $\alpha = 0$ ; this is due to the fact that known cancer genes tend to cluster together in the network [20] and our propagation technique ranks highly the genes close to the genes in  $\mathcal{K}$ .

We also consider uKIN’s performance as compared to an *unguided* walk with the same restart probability  $\alpha = 0.5$ . In this case, the walk selects a neighboring node to move to uniformly at random. The stationary distribution that the walk converges to depends upon the starting locations and the network topology but is independent of the prior information. Such a walk provides a good baseline to judge the impact

the propagated prior information  $q$  has on the performance of our algorithm, and is an approach that has been widely applied [14]. As evident in Figure 2a, an *unguided* walk (purple line) performs considerably worse than uKIN with  $\alpha = 0.5$ , highlighting the importance of  $q$  in *guiding* the walk.

Notably, the trends we observe on GBM hold across all 24 cancers (Figure 2b). For each cancer type, we consider the  $\log_2$  ratio of the AUPRC of the version of uKIN that uses both prior and new information with  $\alpha = 0.5$  to the AUPRC for each of the other variants. For all cancer 24 cancers, when uKIN uses both prior and new information with  $\alpha = 0.5$ , it outperforms the cases when using only prior information (Figure 2b, left) or using only new information (Figure 2b, middle and right). Further, we observe this improvement when using both prior and new information across all cancers for a wide range of  $\alpha$  ( $0.2 < \alpha < 0.8$ , data not shown), clearly demonstrating that using both sources of information is beneficial.

**uKIN is effective in uncovering cancer-relevant genes.** We next evaluate uKIN’s performance in uncovering cancer-relevant genes as compared to several previous methods. These methods do not use any prior knowledge of cancer genes, and any performance differences between uKIN and them may be due either to the use of this important additional source of information or to specific algorithmic differences between the methods. Nevertheless, such comparisons are necessary to get an idea of how well uKIN performs as compared to the current state-of-the-art. All methods are run and AUPRCs computed as described in **Methods**. First, we compare uKIN with  $\alpha = 0.5$  to MutSigCV 2.0 [42], perhaps the most widely used frequency-based approach to identify cancer driver genes. We find that uKIN outperforms MutSigCV 2.0 on 22 of 24 cancer types (Figure 3a). Next, we compare uKIN to three network-based approaches (Figure 3b): Muffinn [43], which considers mutations found in interacting genes; DriverNet [30], which finds driver genes by uncovering sets of somatically mutated genes that are linked to dysregulated genes; and nCOP [39], which examines the per-individual mutational profiles of cancer patients in a biological network. uKIN exhibits superior performance across all cancer types when compared to DriverNet, and outperforms Muffinn in 23 out of 24 cancer types and nCOP in 17 of the 24 cancer types. In many cases, the performance improvements of uKIN are substantial (e.g., more than a 2-fold improvement for 12, 10, 3 and 4 cancer types for MutSigCV, DriverNet, Muffin and nCOP, respectively). We also compare to Hotnet2 [25], whose core algorithmic component is diffusion [28], and as such uKIN is more similar to it than other methods. Hotnet2 does not output a ranked list of genes, so we instead examine the list of genes highlighted by both methods. We find that uKIN exhibits higher precision and recall than Hotnet2 for all cancer types (Suppl. Figure S1); since both uKIN and Hotnet2 are network propagation approaches, these performance improvements illustrate the benefit of using prior information in identifying cancer-relevant genes.

**Robustness tests.** The overall results shown hold when we use different lists of known cancer genes as a gold standard (Suppl. Figure S2a), different numbers of predictions considered when computing AUPRCs (Suppl. Figure S2b), and different networks (Suppl. Figure S2c). Further, we confirm the importance of network structure to uKIN, by running uKIN on two types of randomized networks, degree-preserving and label shuffling, and show that, as expected, overall performance deteriorates across the cancer types (Suppl. Figure S2d); we note that while network structure is destroyed by these randomizations, per-gene mutational information is preserved, and thus highly mutated genes are still output.

We also determine the effect of the amount of prior knowledge for uKIN, and find that while performance increases with larger numbers of genes comprising our prior knowledge, even as few as five prior knowledge genes leads to a  $\sim 4$ -fold improvement over ranking genes by mutational frequency (Suppl. Figure S3a). Finally, we investigate the effect of some incorrect prior knowledge, and find that while uKIN’s performance decreases with more incorrect knowledge, uKIN with  $\alpha = 0.5$  performs reasonably with  $< 20\%$  incorrect annotations (Suppl. Figure S3b).

**Alternate formulations.** We also tested guided diffusion from the somatically mutated genes instead of RWRs (see **Methods**). We empirically find that, for  $\alpha = 0.5$ , diffusion with  $\lambda = 1$  yields nearly identical



per-gene scores on the cancer datasets we tested (GBM and kidney renal cell carcinoma). Similarly, for other  $\alpha$ , we were able to find values of  $\lambda$  such that the RWRs and diffusion have highly similar results. On the other hand, replacing the initial diffusion from the prior knowledge with a RWR (with  $\alpha = 0.5$ ) results in somewhat worse performance (e.g.,  $\sim 10\%$  drop in AUPRC for GBM).

### uKIN highlights infrequently mutated cancer-relevant genes.

A major advantage of network-based methods is that they are able to identify cancer-relevant genes that are not necessarily mutated in large numbers of patients [25]. We next analyze the mutation frequency of genes output by uKIN with  $\alpha = 0.5$ . In particular, for each cancer type, for each gene, we obtain a final score by averaging scores across the 100 runs of uKIN; to prevent “leakage” from the prior knowledge set, if a gene is in the set of prior knowledge genes  $\mathcal{K}$  for a run, this run is not used when determining its final score. We confirm that, for all cancer types, the top scoring genes exhibit diverse mutational rates, and include both frequently and infrequently mutated genes (Suppl. Figure S4).

We next highlight some infrequently mutated genes in GBM that are given high final scores by uKIN (i.e., are predicted as cancer-relevant). For example, *LAND1A* and *SMAD4* are two well known cancer players that are highly ranked by uKIN, and that have mutational rates in GBM that are in the bottom 70% of all genes and are therefore hard to detect with frequency-based approaches. Of uKIN’s top 100 scoring genes, 23 are in the bottom half with respect to mutational rates, and 5 of these are CGCs ( $p < 10^{-2}$ , hypergeometric test). When considering the top scoring 100 genes by uKIN for each cancer type, those that have mutational ranks in the bottom half of all genes are each found to have a statistically significant enrichments of CGC genes. Thus, uKIN provides a means for pulling out cancer genes from the “long tail” [44] of infrequently mutated genes.

In addition to highlighting known cancer genes, uKIN also ranks highly several non-CGC genes that may or may not play a functional role in cancer, as our knowledge of cancer-related genes is incomplete. Among these novel predictions for GBM are *ATXN1*, *SMURF1*, and *CCR3*, all of which have been recently suggested to play a role in cancers [45–47] and are each mutated in less than 5% of the samples. *ATXN1* is a chromatin-binding factor that plays a critical role in the development of spinocerebellar ataxia, a neurodegenerative disorder [48], and mutants of *ATXN1* have been found to stimulate the proliferation of cerebellar stem cells in mice [49]. This is a promising gene for further investigation because glioblastoma is a cancer that usually starts in the cerebrum and the potential role of *ATXN1* in tumorigenesis has only recently been

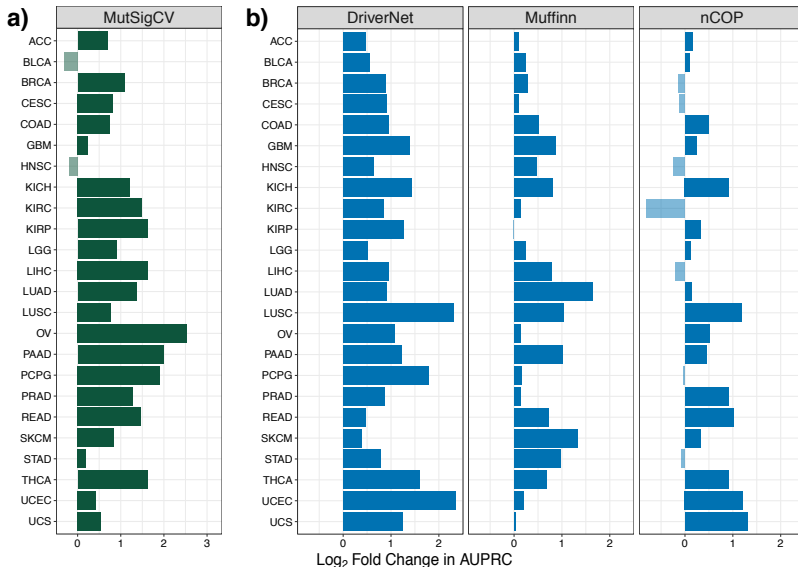


Figure 3: **uKIN is more effective than other methods in identifying known cancer genes.** For each method, for each cancer type, we plot the  $\log_2$  ratio of uKIN’s AUPRC to its AUPRC. **(a)** Comparison of uKIN to MutSigCV 2.0, a state-of-the-art frequency-based approach. uKIN outperforms MutSigCV 2.0 on 22 of the 24 cancer types. **(b)** Comparison of uKIN to DriverNet (left), Muffinn (middle), and nCOP (right). Our approach uKIN outperforms DriverNet on all cancer types, Muffinn on all but one cancer type and nCOP on 17 out of 24 cancer types.

suggested [45]. *SMURF1* and its highly ranked by  $\mathbf{uKIN}$  network-interactor *SMAD1* have already been implicated in the development of several cancers [50]. *SMURF1* also interacts with the nuclear receptor *TLX* whose inhibitory role in glioblastoma has been revealed [51]. Overall, we also find that the top scoring genes by  $\mathbf{uKIN}$  for GBM are enriched in many KEGG pathways and GO terms relevant for cancer, including *microRNAs in cancer*, *cell proliferation*, *choline metabolism in cancer* and *apoptosis* (Bonferroni-corrected  $p < 0.001$ , hypergeometric test).

### Cancer-type specific prior knowledge yields better performance.

In several cases, CGC genes are annotated with the specific cancers they play driver roles in. We next test how  $\mathbf{uKIN}$ 's performance changes when using such highly specific prior knowledge. We consider four cancer types, GBM, breast invasive carcinoma (BRCA), skin cutaneous carcinoma (SKCM), and thyroid carcinoma (THCA), with 33, 32, 42 and 29 CGC genes annotated to them, respectively. We repeatedly split each of these sets of genes in half, and use half as the set  $\mathcal{K}$  of prior knowledge, and the other half as the set  $\mathcal{H}$  to test performance.

We first use knowledge consisting of genes specific to a cancer type of interest together with the TCGA data for that cancer to uncover that cancer's specific drivers. Given the small number of

genes annotated to each cancer, we assess performance by, for each of these genes, computing the rank of its score by  $\mathbf{uKIN}$  over the splits where these genes are in  $\mathcal{H}$ . Next, for the *same* cancer type, we use a set  $\mathcal{K}$  corresponding to a *different* cancer type as prior knowledge (excluding any genes that are annotated to the *original* cancer type) while still trying to uncover the genes in the *original* cancer of interest (i.e., using TCGA mutational data and  $\mathcal{H}$  belonging to the *original* cancer type). That is, we are testing the performance of  $\mathbf{uKIN}$  when using knowledge corresponding to a different cancer type. For all four cancer types, we find that performance is best when  $\mathbf{uKIN}$  uses prior knowledge for the same cancer type (Figure 4a), as genes in  $\mathcal{H}$  appear higher in the list of genes output by  $\mathbf{uKIN}$ . This suggests that  $\mathbf{uKIN}$  can utilize cancer-type specific knowledge and highlights the benefits of having accurate prior information.

**Application to identify disease genes for complex inherited disorders.** A major advantage of our method is that it can be easily applied in diverse settings. As proof of concept, we apply  $\mathbf{uKIN}$  to detect disease genes

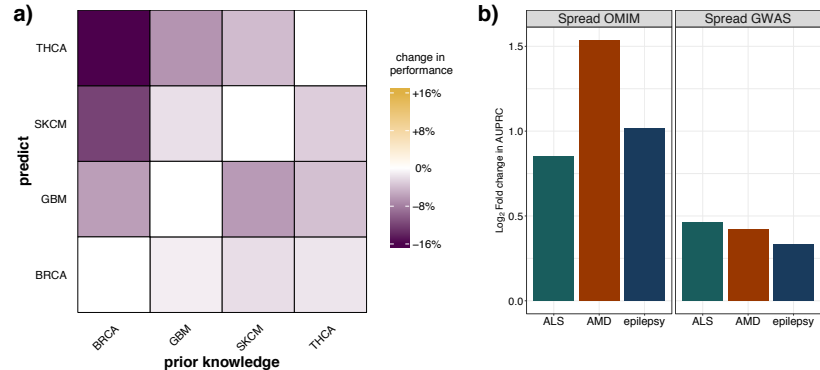


Figure 4: **(a) Use of cancer-type specific knowledge improves performance.**

For four cancer types, BRCA, GBM, SKCM, and THCA, we consider the performance of  $\mathbf{uKIN}$  with  $\alpha = 0.5$  when using TCGA mutational data for that cancer type with prior knowledge consisting of genes known to be driver in that cancer type, as compared to performance when the prior knowledge set consists of genes that are annotated as driver only for one of the other three cancer types. For each cancer, performance is measured by the average ranking by  $\mathbf{uKIN}$  of genes known to be driver for that cancer. For all combinations of possible prior knowledge sets ( $x$ -axis) and specific cancer gene sets that we wish to recover ( $y$ -axis), using prior knowledge from another cancer (off diagonal entries) leads to a decrease in performance as compared to the corresponding pairs (diagonal entries), as measured by the increase in  $\mathbf{uKIN}$ 's average ranking of genes we aimed to uncover. **(b)  $\mathbf{uKIN}$  is effective in identifying complex disease genes.** We demonstrate the versatility of the  $\mathbf{uKIN}$  framework by integrating OMIM and GWAS data for three complex diseases, *ALS*, *epilepsy* and *AMD*. For each disease, we compare  $\mathbf{uKIN}$ 's performance when using OMIM annotated genes as prior information and GWAS hits as new information with  $\alpha = 0.5$ , to baseline versions that propagate only information via diffusion from OMIM (left) or GWAS studies (right). In all cases, we plot the  $\log_2$  ratio of the AUPRC obtained by  $\mathbf{uKIN}$  using both prior and new information to the baseline methods.

for three complex diseases: *AMD*, *ALS* and *epilepsy*. For each disease, we randomly split in half the OMIM database’s [36] list of genes associated with the disease 100 times to form the set of prior knowledge  $\mathcal{K}$  and the hidden set  $\mathcal{H}$ . We use the GWAS catalogue list of genes with their corresponding  $p$ -values to form the set  $\mathcal{M}$ . For all three diseases,  $\text{uKIN}$  combining both GWAS and OMIM sources of information ( $\alpha = 0.5$ ) performs better than diffusing the signal with  $\lambda = 1$  using only knowledge from OMIM (Figure 4b, left panel). For each of these diseases, there is virtually no overlap between the GWAS hits  $\mathcal{M}$  and a set of OMIM genes  $\mathcal{H}$ ; simply sorting genes by their significance in GWAS studies (i.e.,  $\text{uKIN}$  with  $\alpha = 1$ ) results in AUPRC of 0. Instead, we spread information from the set of GWAS genes  $\mathcal{M}$  in the same fashion as from OMIM and observe again that using this single source of information alone does not work as well as  $\text{uKIN}$ ’s using both GWAS and OMIM information together (Figure 4b, right panel).

## Discussion

In this paper, we have shown that  $\text{uKIN}$ , a network propagation method that incorporates both existing knowledge as well as new information, is a highly effective and versatile approach for uncovering disease genes. Our method is based upon the intuition that prior knowledge of disease-relevant genes can be used to guide the way information from new data is spread and interpreted in the context of biological networks. Because  $\text{uKIN}$  uses prior knowledge, it has higher precision than other state-of-the-art methods in detecting known cancer genes. Further, it excels at highlighting infrequently mutated genes that are nevertheless relevant for cancer. Additionally, we have shown that  $\text{uKIN}$  can be applied to discover genes relevant for other complex diseases as well.

The framework presented here can be extended in a number of natural ways. First, in addition to positive knowledge of known disease genes, we may also have “negative” knowledge of genes that are not involved in the development of a given disease. These genes can propagate their “negative” information, thereby biasing the random walk to move away from their respective modules and perhaps further enhancing the performance of our method. Second,  $\text{uKIN}$  is likely to benefit from incorporating edge weights that reflect the reliability of interactions between proteins; these weights will have an impact on both the propagation of prior knowledge as well as the guided random walks. Third, since a recent study [52] has shown that contrasting cancer mutation data with natural germline variation data helps boost the true disease signal by downgrading genes that vary frequently in nature,  $\text{uKIN}$ ’s performance may benefit from scaling the starting probabilities of the new putatively implicated genes to account for their variation in healthy populations. Fourth, while here we have demonstrated how  $\text{uKIN}$  can use cancer-type specific knowledge, cancers of the same type can often be grouped into distinct subtypes, and such highly-detailed knowledge may improve  $\text{uKIN}$ ’s performance even further. Finally, we note that network propagation approaches have been applied to non-disease settings as well, including biological process prediction [53, 54]. We conjecture that our guided network propagation approach will additionally be useful in other scenarios in computational biology, including where new data (e.g., arising from functional genomics screens) need to be interpreted in the context of what is already known about a biological process of interest.

In conclusion,  $\text{uKIN}$  is a flexible and effective method that handles diverse types of new information. As our knowledge of disease-associated genes continues to grow and be refined, and as new experimental data becomes more abundant, we expect that the power of  $\text{uKIN}$  for accurately prioritizing disease genes will continue to increase.

## References

- [1] 1000 Genomes Project Consortium and others. A global reference for human genetic variation. *Nature*, 526(7571):68, 2015.
- [2] TCGA Research Network. <http://cancergenome.nih.gov/>.
- [3] Karczewski KJ, Francioli LC, Tiao G, Cummings BB, Alföldi J, Wang Q, *et al.* Variation across 141,456 human exomes and genomes reveals the spectrum of loss-of-function intolerance across human protein-coding genes. *bioRxiv*, 2019.
- [4] Kim YA, Przytycka TM. Bridging the gap between genotype and phenotype via network approaches. *Frontiers in genetics*, 3:227, 2013.
- [5] Goh KI, Cusick ME, Valle D, Childs B, Vidal M, Barabási AL. The human disease network. *Proceedings of the National Academy of Sciences*, 104(21):8685–8690, 2007.
- [6] Barabási AL, Gulbahce N, Loscalzo J. Network medicine: a network-based approach to human disease. *Nature reviews genetics*, 12(1):56, 2011.
- [7] Cowen L, Ideker T, Raphael BJ, Sharan R. Network propagation: a universal amplifier of genetic associations. *Nature Reviews Genetics*, 18(9):551, 2017.
- [8] Ozturk K, Dow M, Carlin DE, Bejar R, Carter H. The emerging potential for network analysis to inform precision cancer medicine. *Journal of molecular biology*, 430(18):2875–2899, 2018.
- [9] Hartwell L, Hopfield J, Leibler S, Murray A. From molecular to modular cell biology. *Nature*, 402:C47–52, 1999.
- [10] Spirin V, Mirny LA. Protein complexes and functional modules in molecular networks. *Proc Natl Acad Sci USA*, 100:12123–12128, 2003.
- [11] Oti M, Brunner HG. The modular nature of genetic diseases. *Clinical genetics*, 71(1):1–11, 2007.
- [12] Gandhi T, Zhong J, Mathivanan S, Karthick L, Chandrika K, Mohan SS, Sharma S, Pinkert S, Nagaraju S, Periaswamy B, *et al.* Analysis of the human protein interactome and comparison with yeast, worm and fly interaction datasets. *Nature genetics*, 38(3):285, 2006.
- [13] Krauthammer M, Kaufmann CA, Gilliam TC, Rzhetsky A. Molecular triangulation: bridging linkage and molecular-network information for identifying candidate genes in Alzheimer’s disease. *Proceedings of the National Academy of Sciences*, 101(42):15148–15153, 2004.
- [14] Köhler S, Bauer S, Horn D, Robinson PN. Walking the interactome for prioritization of candidate disease genes. *The American Journal of Human Genetics*, 82(4):949–958, 2008.
- [15] Chen J, Aronow B, Jegga A. Disease candidate gene identification and prioritization using protein interaction networks. *BMC Bioinformatics*, 10, 2009.
- [16] Vanunu O, Magger O, Ruppin E, Shlomi T, Sharan R. Associating genes and protein complexes with disease via network propagation. *PLoS computational biology*, 6(1):e1000641, 2010.
- [17] Navlakha S, Kingsford C. The power of protein interaction networks for associating genes with diseases. *Bioinformatics*, 26(8):1057–1063, 2010.
- [18] Erten S, Bebek G, Ewing RM, Koyuturk M. DADA: Degree-aware algorithms for network-based disease gene prioritization. *BioData Min*, 4:19, 2011.
- [19] Smedley D, Khler S, Czeschik JC, Amberger J, Bocchini C, Hamosh A, Veldboer J, Zemojtel T, Robinson P. Walking the interactome for candidate prioritization in exome sequencing studies of Mendelian diseases. *Bioinformatics*, 30:3215–3222, 2014.

- [20] Cerami E, Demir E, Schultz N, Taylor BS, Sander C. Automated network analysis identifies core pathways in glioblastoma. *PLoS ONE*, 5(2):e8918, 2010.
- [21] Vandin F, Upfal E, Raphael BJ. Algorithms for detecting significantly mutated pathways in cancer. *Journal of Computational Biology*, 18(3):507–522, 2011.
- [22] Lee I, Blom UM, Wang PI, Shim JE, Marcotte EM. Prioritizing candidate disease genes by network-based boosting of genome-wide association data. *Genome research*, 21(7):1109–1121, 2011.
- [23] Babaei S, Hulsman M, Reinders M, de Ridder J. Detecting recurrent gene mutation in interaction network context using multi-scale graph diffusion. *BMC Bioinformatics*, 14:29, 2013.
- [24] Jia P, Zhao Z. Varwalker: personalized mutation network analysis of putative cancer genes from next-generation sequencing data. *PLoS Comput Biol*, 10(2):e1003460, 2014.
- [25] Leiserson MDM, Vandin F, Wu HT, Dobson JR, Eldridge JV, Thomas JL, Papoutsaki A, Kim Y, Niu B, McLellan M, Lawrence MS, Gonzalez-Perez A, Tamborero D, Cheng Y, Ryslik GA, Lopez-Bigas N, Getz G, Ding L, Raphael BJ. Pan-cancer network analysis identifies combinations of rare somatic mutations across pathways and protein complexes. *Nature Genetics*, 47:106–114, 2015.
- [26] Carlin D, Fong S, Qin Y, Jia T, Huang J, Bao B, Zhang C, Ideker T. A fast and flexible framework for network-assisted genomic association. *iScience*, 16:155–161, 2019.
- [27] Lawrence M, Stojanov P, Polak P, Kryukov G, Cibulskis K, Sivachenko A, *et al.* Mutational heterogeneity in cancer and the search for new cancer-associated genes. *Nature*, 499:214–218, 2013.
- [28] Qi Y, Suhail Y, Lin Yy, Boeke JD, Bader JS. Finding friends and enemies in an enemies-only network: a graph diffusion kernel for predicting novel genetic interactions and co-complex membership from yeast genetic interactions. *Genome research*, 18:1991–2004, 2008.
- [29] Kim Y, Wuchty S, Przytycka T. Identifying causal genes and dysregulated pathways in complex diseases. *PLoS Comput Biol*, 7:e1001095, 2011.
- [30] Bashashati A, Haffari G, Ding J, Ha G, Lui K, Rosner J, Huntsman DG, Caldas C, Aparicio SA, Shah SP. DriverNet: uncovering the impact of somatic driver mutations on transcriptional networks in cancer. *Genome biology*, 13(12):R124, 2012.
- [31] Paull EO, Carlin DE, Niepel M, Sorger PK, Haussler D, Stuart JM. Discovering causal pathways linking genomic events to transcriptional states using Tied Diffusion Through Interacting Events (TieDIE). *Bioinformatics*, 29(21):2757–2764, 2013.
- [32] Shrestha R, Hodzic E, Yeung J, Wang K, Sauerwald T, Dao P, Anderson S, Beltran H, Rubin MA, Collins CC, *et al.* Hitndrive: multi-driver gene prioritization based on hitting time. In *International Conference on Research in Computational Molecular Biology*, pages 293–306. Springer, 2014.
- [33] Ruffalo M, Koyutrk M, Sharan R. Network-based integration of disparate omic data to identify “silent players” in cancer. *PLOS Computational Biology*, 11:e1004595, 2015.
- [34] Shi K, Gao L, Wang B. Discovering potential cancer driver genes by an integrated network-based approach. *Molecular Biosystems*, 12:2921–2931, 2016.
- [35] Futreal PA, Coin L, Marshall M, Down T, Hubbard T, Wooster R, Rahman N, Stratton MR. A census of human cancer genes. *Nat Rev Cancer*, 4(3):177–83, 2004.
- [36] Online Mendelian Inheritance in Man, OMIM®, 2000.
- [37] Prasad TK, Goel R, Kandasamy K, Keerthikumar S, Kumar S, Mathivanan S, Telikicherla D, Raju R, Shafreen B, Venugopal A, *et al.* Human protein reference database–2009 update. *Nucleic acids research*, 37(suppl 1):D767–D772, 2009.

- [38] Stark C, Breitkreutz BJ, Reguly T, Boucher L, Breitkreutz A, Tyers M. BioGRID: a general repository for interaction datasets. *Nucleic acids research*, 34(suppl 1):D535–D539, 2006.
- [39] Hristov BH, Singh M. Network-based coverage of mutational profiles reveals cancer genes. *Cell systems*, 5(3):221–229, 2017.
- [40] Cao M, Zhang H, Park J, Daniels NM, Crovella ME, Cowen LJ, Hescott B. Going the distance for protein function prediction: a new distance metric for protein interaction networks. *PloS one*, 8(10):e76339, 2013.
- [41] Buniello A, MacArthur JAL, Cerezo M, Harris LW, Hayhurst J, Malangone C, McMahon A, Morales J, Mountjoy E, Sollis E, *et al.* The NHGRI-EBI GWAS Catalog of published genome-wide association studies, targeted arrays and summary statistics 2019. *Nucleic acids research*, 47(D1):D1005–D1012, 2018.
- [42] Lawrence MS, Stojanov P, Polak P, Kryukov GV, Cibulskis K, Sivachenko A, Carter SL, Stewart C, Mermel CH, Roberts SA, *et al.* Mutational heterogeneity in cancer and the search for new cancer-associated genes. *Nature*, 499(7457):214–218, 2013.
- [43] Cho A, Shim JE, Kim E, Supek F, Lehner B, Lee I. Muffinn: cancer gene discovery via network analysis of somatic mutation data. *Genome Biology*, 17(1):129, 2016.
- [44] Garraway LA, Lander ES. Lessons from the cancer genome. *Cell*, 153(1):17–37, 2013.
- [45] Kang AR, An HT, Ko J, Choi EJ, Kang S. Ataxin-1 is involved in tumorigenesis of cervical cancer cells via the EGFR–RAS–MAPK signaling pathway. *Oncotarget*, 8(55):94606, 2017.
- [46] Li H, Xiao N, Wang Y, Wang R, Chen Y, Pan W, Liu D, Li S, Sun J, Zhang K, *et al.* Smurf1 regulates lung cancer cell growth and migration through interaction with and ubiquitination of PIPKI $\gamma$ . *Oncogene*, 36(41):5668, 2017.
- [47] Lee YS, Kim SY, Song SJ, Hong HK, Lee Y, Oh BY, Lee WY, Cho YB. Crosstalk between CCL7 and CCR3 promotes metastasis of colon cancer cells via erk-jnk signaling pathways. *Oncotarget*, 7(24):36842, 2016.
- [48] Rousseaux MW, Tschumperlin T, Lu HC, Lackey EP, Bondar VV, Wan YW, Tan Q, Adamski CJ, Friedrich J, Twaroski K, *et al.* ATXN1-CIC complex is the primary driver of cerebellar pathology in spinocerebellar ataxia type 1 through a gain-of-function mechanism. *Neuron*, 97(6):1235–1243, 2018.
- [49] Edamakanti CR, Do J, Didonna A, Martina M, Opal P. Mutant ataxin1 disrupts cerebellar development in spinocerebellar ataxia type 1. *The Journal of clinical investigation*, 128(6):2252–2265, 2018.
- [50] Yang D, Hou T, Li L, Chu Y, Zhou F, Xu Y, Hou X, Song H, Zhu K, Hou Z, *et al.* Smad1 promotes colorectal cancer cell migration through Ajuba transactivation. *Oncotarget*, 8(66):110415, 2017.
- [51] Johansson E, Zhai Q, Zeng Zj, Yoshida T, Funa K. Nuclear receptor TLX inhibits TGF- $\beta$  signaling in glioblastoma. *Experimental cell research*, 343(2):118–125, 2016.
- [52] Przytycki PF, Singh M. Differential analysis between somatic mutation and germline variation profiles reveals cancer-related genes. *Genome medicine*, 9(1):79, 2017.
- [53] Wang P, Marcotte E. It’s the machine that matters: Predicting gene function and phenotype from protein networks. *J Proteomics*, 73:2277–2289, 2011.
- [54] Nabieva E, Jim K, Agarwal A, Chazelle B, Singh M. Whole-proteome prediction of protein function via graph-theoretic analysis of interaction maps. *Bioinformatics*, 21 Suppl. 1:i302–i310, 2005.
- [55] Hofree M, Carter H, Kreisberg JF, Bandyopadhyay S, Mischel PS, Friend S, Ideker T. Challenges in identifying cancer genes by analysis of exome sequencing data. *Nature Communications*, 7, 2016.
- [56] Vogelstein B, Papadopoulos N, Velculescu VE, Zhou S, Diaz J L A, Kinzler KW. Cancer genome landscapes. *Science*, 339(6127):1546–58, 2013.

## **Supplementary Figures and Tables**

The following pages contain 1 table and 4 supplementary figures that support the findings of the main paper.

Cancer Symbol	Cancer Type	Number of Patients	Number of Mutated Genes		
			Total	Average	Cut off
ACC	Adrenocortical carcinoma	76	2068	32.1	80
BLCA	Bladder Urothelial Carcinoma	196	11407	135.7	300
BRCA	Breast invasive carcinoma	882	10813	27	80
CESC	Cervical squamous cell carcinoma and endocervical adenocarcinoma	173	6907	63	200
COAD	Colon adenocarcinoma	153	6521	74.4	150
GBM	Glioblastoma multiforme	278	7250	46.8	80
HNSC	Head and Neck squamous cell carcinoma	435	13048	87.9	200
KICH	Kidney Chromophobe	64	661	11	50
KIRC	Kidney renal clear cell carcinoma	416	9212	40.9	100
KIRP	Kidney renal papillary cell carcinoma	166	5687	47.7	100
LGG	Brain Lower Grade Glioma	451	7130	28.8	60
LIHC	Liver hepatocellular carcinoma	196	7705	67.3	200
LUAD	Lung adenocarcinoma	487	15481	172.8	500
LUSC	Lung squamous cell carcinoma	167	12264	212	500
OV	Ovarian serous cystadenocarcinoma	138	3390	30.7	80
PAAD	Pancreatic adenocarcinoma	124	3228	36.8	100
PCPG	Pheochromocytoma and Paraganglioma	183	1819	11.7	30
PRAD	Prostate adenocarcinoma	238	4792	28.1	50
READ	Rectum adenocarcinoma	34	1214	40.7	150
SKCM	Skin Cutaneous Melanoma	329	14748	240.1	1000
STAD	Stomach adenocarcinoma	242	10595	103.5	500
THCA	Thyroid carcinoma	401	2268	7.4	30
UCEC	Uterine Corpus Endometrial Carcinoma	155	4282	38.8	100
UCS	Uterine Carcinosarcoma	54	1787	38.9	80

Table S1: **TCGA dataset and statistics.** We list the 24 cancer types studied along with their abbreviations. For each cancer type, we give the total number of patient samples considered after highly mutated samples are filtered out, the total number of mutated genes across these samples, the average number of mutated genes across all samples, and the cutoff on the number of mutated genes within a sample that was used to filter samples.



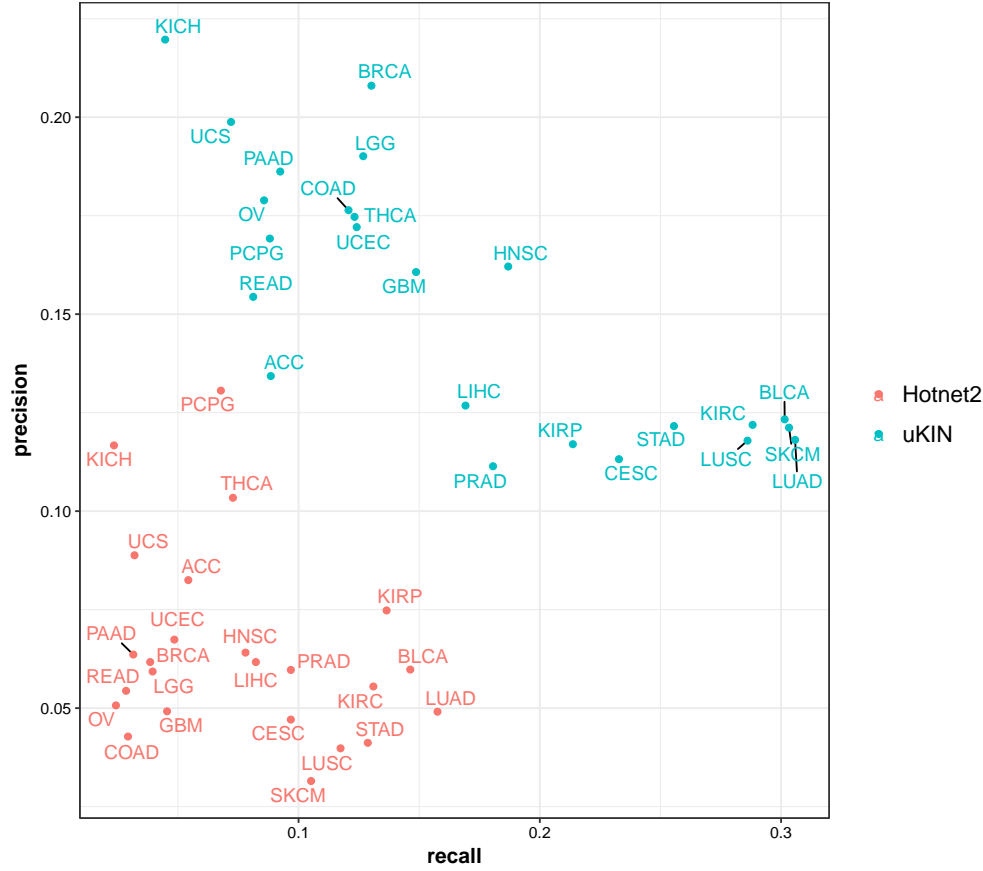


Figure S1: **Comparison between uKIN and Hotnet2.** For each cancer type, we compute the precision and recall of the genes returned by uKIN with  $\alpha=0.5$  and Hotnet2. Hotnet2 is run with default parameters (100 permuted networks, and  $\beta = 0.2$  for the restart probability for the insulated heat diffusion process). Hotnet2 outputs a set of genes predicted to be cancer-relevant, and these genes are not ranked. Thus, for uKIN, we consider the same number of top scoring genes as output by Hotnet2. uKIN exhibits both higher precision and higher recall than Hotnet2 across all 24 cancer types.

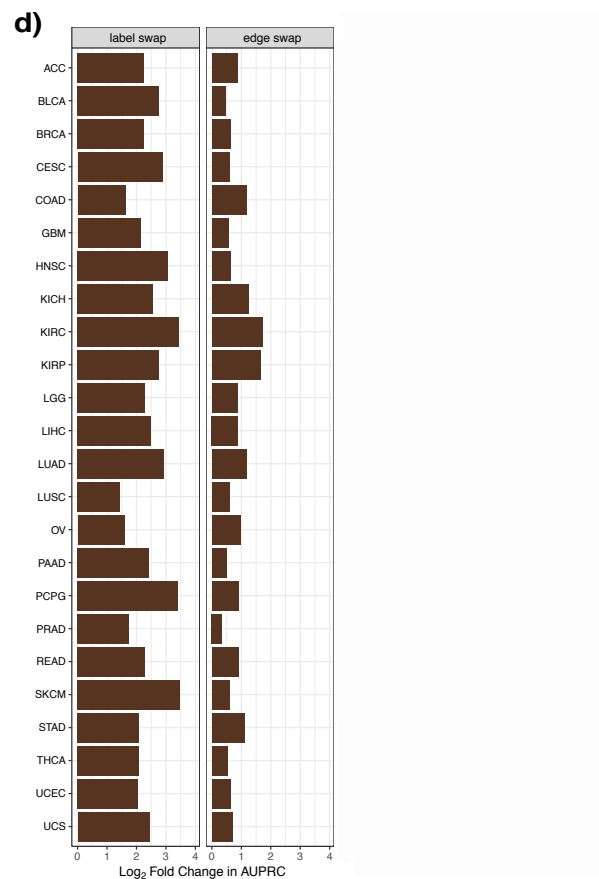
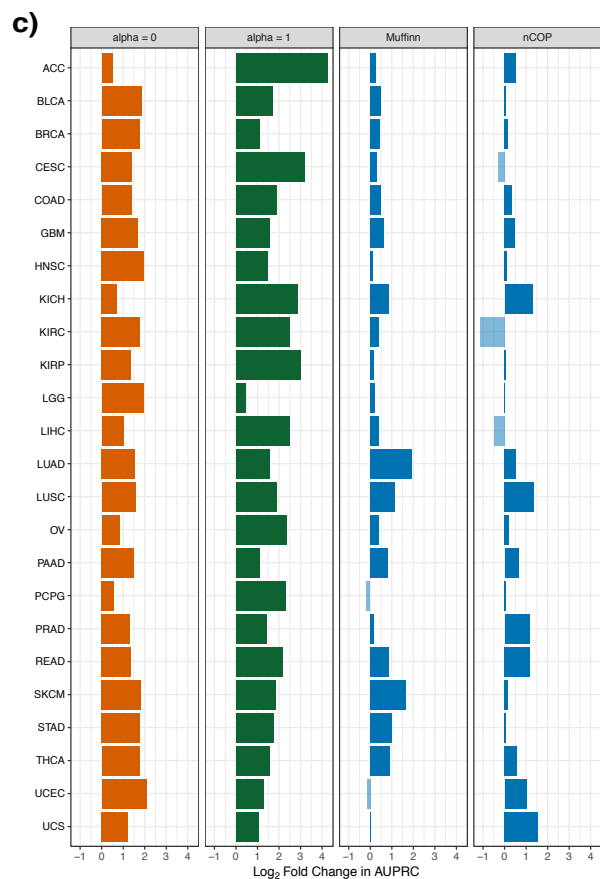
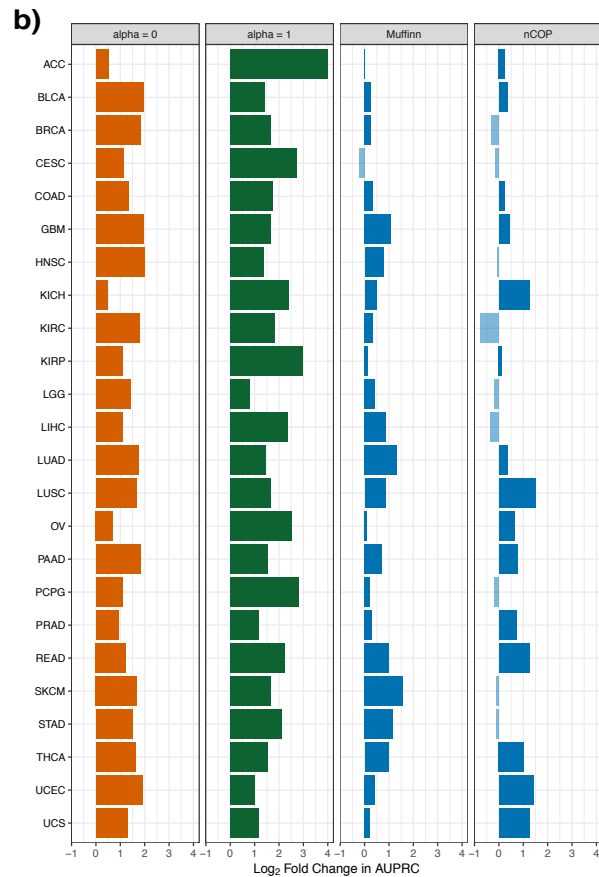
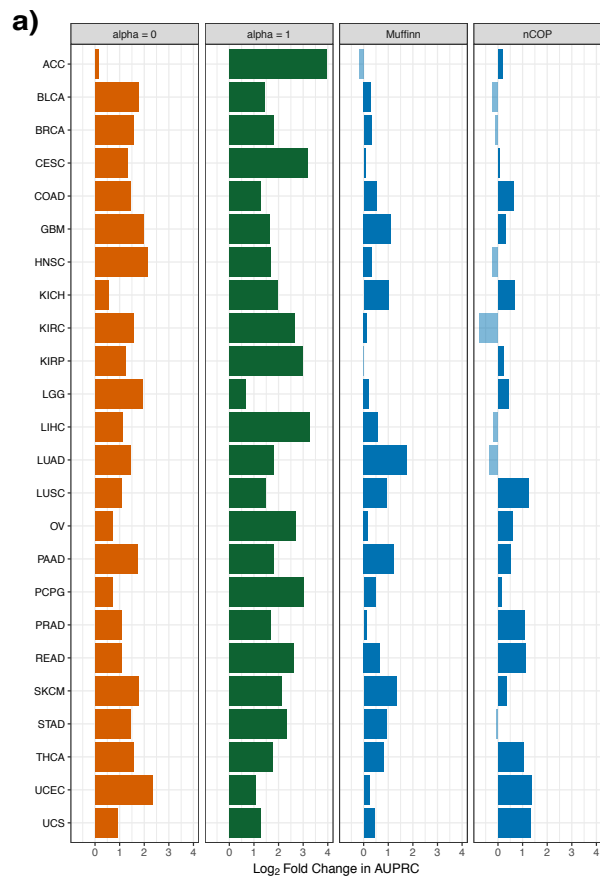


Figure S2: **Robustness of  $\mathbf{uKIN}$ .** **(a)** To make sure that the results reported for  $\mathbf{uKIN}$  in Figures 2 and 3 are robust with respect to the set of labelled cancer genes  $\mathcal{H}$ , instead of randomly sampling 400 genes from the Cancer Gene Census (CGC) list, we form  $\mathcal{H}$  using genes from other sources. Specifically, we aggregate the cancer genes provided by Hofree et al. in [55] (which they obtained by querying the UniprotKB database for the keyword-terms ‘proto-oncogene,’ ‘oncogene’ and ‘tumoursuppressor’ gene) and Vogelstein et al. [56], excluding any genes present in the set of prior knowledge  $\mathcal{K}$ . Log-fold AUPRCs are computed as described in the main text. The results are consistent with those shown in Figures 2 and 3 based on the CGC list and show the superior performance of  $\mathbf{uKIN}$  as compared to the other methods in recapitulating known cancer genes. **(b)** To make sure that the results reported for  $\mathbf{uKIN}$  in Figures 2 and 3 are robust with respect to number of genes used in evaluation, we compute AUPRCs using the top 50 predicted genes. The results are consistent with those shown in Figures 2 and 3 which use the top 100 predicted genes, and show the superior performance of  $\mathbf{uKIN}$  as compared to the baselines and other methods in recapitulating known cancer genes. The results are also consistent when computing AUPRC’s using 150 genes (data not shown). **(c)** To make sure that our method is robust with respect to the specific network utilized, we repeat our entire analysis procedure for  $\mathbf{uKIN}$  with  $\alpha = 0.5$  using the Biogrid network. The results are consistent with those shown in Figures 2 and 3, based on the HPRD network. **(d)** To make sure our method utilizes network structure appropriately, we also consider performance of  $\mathbf{uKIN}$  on the real HPRD network as compared to randomized HPRD networks. In the left panel, we use a node label shuffling randomization where the network structure is maintained but gene names are swapped (thereby genes can have very different numbers of interactions in the randomizations). In the right panel, we use a classic degree-preserving randomization (edge swapping). For each of the 24 cancers, we compute the  $\log_2$  ratio of the area under the precision recall curve using  $\mathbf{uKIN}$  with  $\alpha = 0.5$  on the real network and on the randomized network and show the average over 10 different randomizations. Performance, as expected, is worse for both randomizations across all cancers. We note that significant cancer-relevant information is retained in these randomized networks. In particular, in both types of network randomizations, we maintain the relationships between genes and the samples that they are found to be somatically mutated in. Thus, some highly mutated CGC genes may still be output by  $\mathbf{uKIN}$  when running on randomized networks.

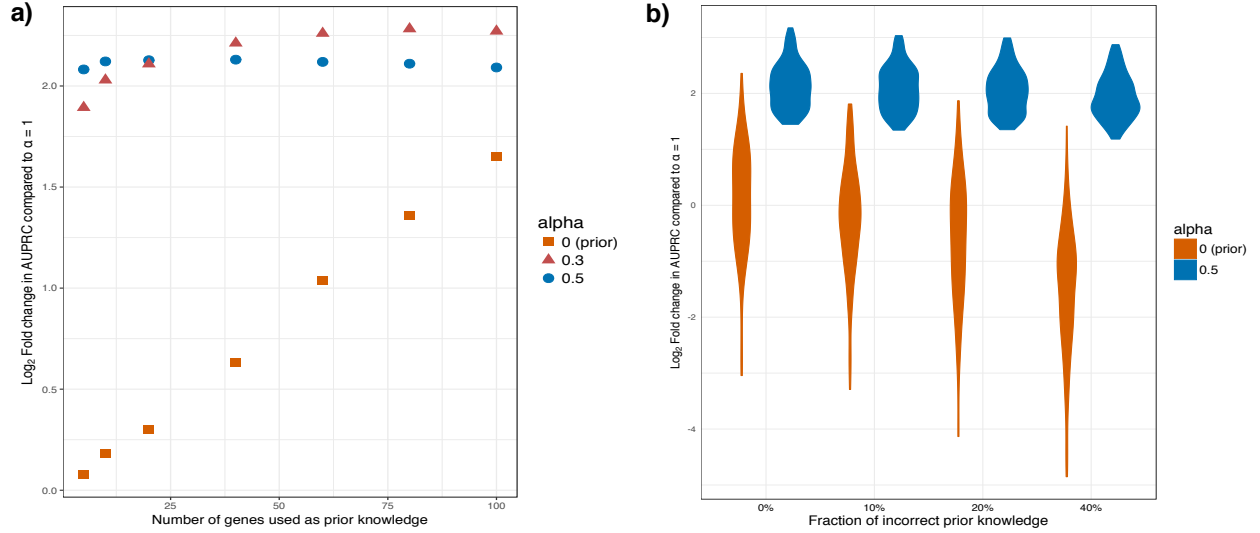
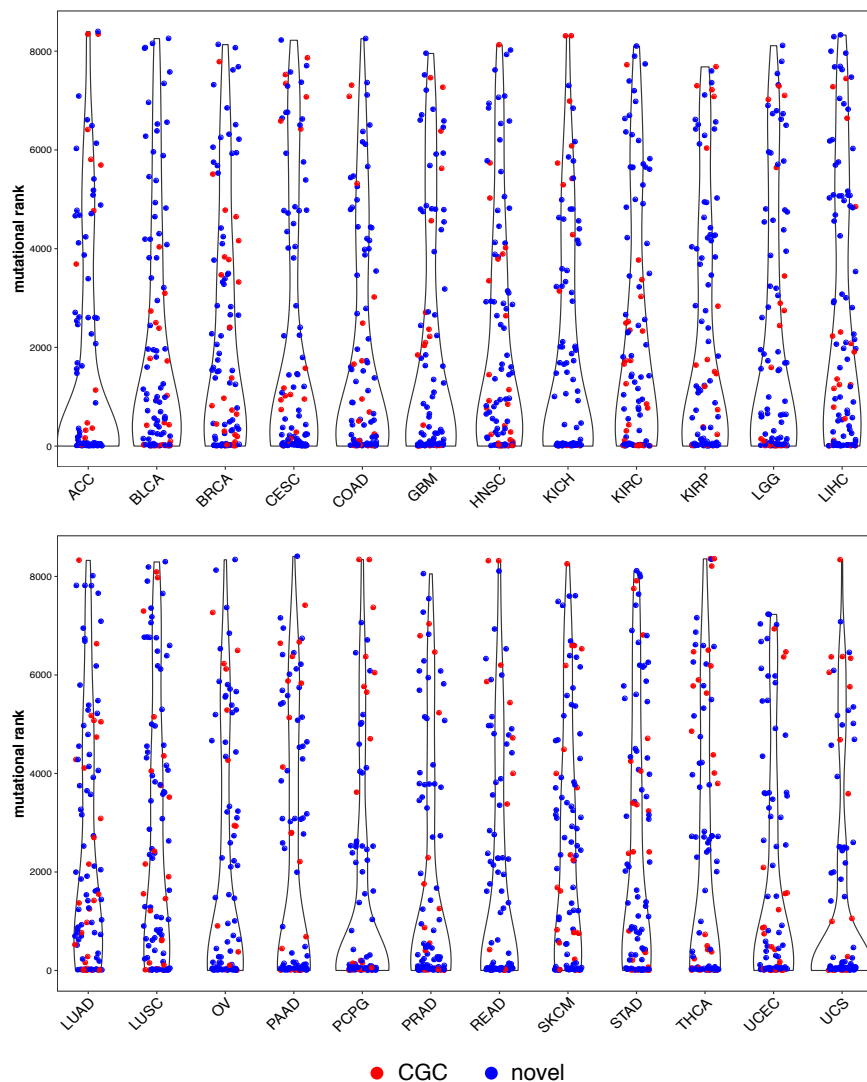


Figure S3: **(a) uKIN benefits from more knowledge.** As we consider larger numbers of genes comprising the set of prior knowledge ( $|\mathcal{K}| = 5, 10, 20, 40, \dots, 100$ ), we examine the ability of uKIN to uncover CGC genes in the same fixed set  $\mathcal{H}$  when using  $\alpha = 0.5$  (blue triangles),  $\alpha = 0.3$  (pink circles) or  $\alpha = 0$  (orange squares). uKIN is run on the HPRD network with the kidney renal clear cell carcinoma (KIRC) dataset. We show the  $\log_2$  ratio, averaged over 100 runs, of the AUPRC of each version of uKIN to the AUPRC for  $\alpha = 1$  which is constant across all possible  $\mathcal{K}$  (and corresponds to the case where genes are ranked by mutational frequency). For small  $\mathcal{K}$ ,  $\alpha = 0$  performs poorly as is expected; as the prior knowledge available increases so does the performance. For both  $\alpha = 0.3$  and  $\alpha = 0.5$ , an increase in the size of  $\mathcal{K}$  leads to an initial increase in the performance but eventually performance plateaus. When limited prior knowledge is available ( $|\mathcal{K}| < 20$ ),  $\alpha = 0.5$ , which uses more of the new information, does better than  $\alpha = 0.3$ , which relies more on using prior knowledge. When prior knowledge is abundant ( $|\mathcal{K}| > 40$ ), uKIN with  $\alpha = 0.3$  outperforms  $\alpha = 0.5$ . As the number of genes comprising the set of prior knowledge increases, spreading information just from those genes ( $\alpha = 0$ ) improves in performance. This is consistent with the observed clustering of CGC genes within biological networks [20]. However, even when propagating information from 100 known cancer genes, the performance is worse than that when integrating it with new information (with either  $\alpha = 0.3$  or  $\alpha = 0.5$ , Figure 3a). **(b) uKIN is robust to small amounts of erroneous knowledge.** We replace a fraction of the CGCs in the set of prior knowledge genes  $\mathcal{K}$  with non-cancerous genes chosen uniformly at random from the set of non-CGC genes in the network. We consider the performance for uKIN with  $\alpha = 0$  and  $\alpha = 0.5$  when 0%, 10%, 20% and 30% of the prior knowledge genes are replaced with non-cancer genes. 100 randomizations are performed at each level of incorrect knowledge. For each run, performance is measured as the  $\log_2$  ratio of the AUPRC of uKIN (with either  $\alpha = 0$  or  $\alpha = 0.5$ ) to the AUPRC for the case where uKIN is run with  $\alpha = 1$  (which is constant). uKIN is run on the HPRD network with KIRC dataset with 20 CGC genes comprising the prior knowledge. Violin plots of this measure are shown for  $\alpha = 0$  (orange) and  $\alpha = 0.5$  (blue), jittered around the 0%, 10%, 20% and 30% tick marks. At  $\alpha = 0.5$ , while performance steadily decreases, uKIN remains robust to some incorrect knowledge ( $\leq 20\%$ ). As expected, for  $\alpha = 0$ , the decrease is more notable even when 10% of the prior knowledge is incorrect because in that case uKIN uses only prior knowledge.



**Figure S4: uKIN identifies rarely mutated genes.** To illustrate uKIN's ability to predict genes as cancer-relevant cancer even if they are mutated across fewer numbers of individuals, we consider mutation rates of uKIN's top scoring genes. For each cancer type, we run uKIN 100 times with  $\alpha = 0.5$  and 20 genes as prior knowledge (see **Methods**). For each gene, its final score is obtained by averaging its scores (arising from the stationary distributions) across the runs; if a gene is in the set of prior knowledge genes  $\mathcal{K}$  for a run, this run is not considered for its final score. For each of the 100 genes with highest final scores, we consider the rank of its mutation rate ( $y$ -axis). The mutation rate of a gene is computed as the number of observed somatic missense and nonsense mutations across tumors of that cancer type, divided by the number of amino acids in the encoded protein. Then, for each cancer type, genes are ranked by mutation rate where the gene with the highest mutation rate is given the lowest rank. Known CGC genes are in red and novel predictions in blue. The top predictions consist of many heavily mutated genes (i.e., those with low ranks), but uKIN is also able to uncover known cancer genes with very low mutational ranks (red dots towards the top).